

Lawrence Berkeley National Laboratory

LBL Publications

Title

CO adsorption on Pd(100) studied by multimodal ambient pressure X-ray photoelectron and infrared reflection absorption spectroscopies

Permalink

<https://escholarship.org/uc/item/55j958df>

Authors

Head, Ashley R
Karslıoğlu, Osman
Gerber, Timm
et al.

Publication Date

2017-11-01

DOI

10.1016/j.susc.2017.08.009

Peer reviewed

CO Adsorption on Pd(100) Studied by Multimodal Ambient Pressure X-ray Photoelectron and Infrared Reflection Absorption Spectroscopies

Ashley R. Head,¹ Osman Karshioğlu,¹ Timm Gerber,¹ Yi Yu,^{1,2} Lena Trotochaud,¹ Joseph Raso,¹ Philipp Kerger,^{1,3} Hendrik Bluhm^{1,4,*}

¹*Chemical Sciences Division and ⁴Advanced Light Source, Lawrence Berkeley National Laboratory, Berkeley CA 94720*

²*Department of Chemistry and Biochemistry, University of Maryland, College Park, MD 20742*

³*Department of Interface Chemistry and Surface Engineering, Max Planck Institute for Iron Research, D-40237 Düsseldorf, Germany.*

*E-mail: hbluhm@lbl.gov

Abstract

The adsorption of CO on Pd(100) was investigated using simultaneous ambient pressure X-ray photoelectron spectroscopy (APXPS) and infrared reflection absorption infrared spectroscopy (IRRAS). The measurements were performed as a function of CO partial pressures from ultra-high vacuum to 0.5 Torr. Total CO coverages estimated from the complementary APXPS and IRRAS measurements are in good agreement. A signal for atop CO, which is uncommon for Pd(100), was observed in the IRRAS data and was used to identify the C 1s binding energy of this species. Discerning this binding configuration of CO on the Pd(100) surface at elevated pressures has significance for catalytic reactions involving CO, where bridging CO is often the only configuration considered. We also detail the combined APXPS/IRRAS instrumentation and discuss ways to improve these multimodal measurements, which should have wide applicability across many areas of surface and interface science.

Keywords

bridging CO, atop CO, surface coverage, IRRAS, APXPS

Introduction

The interaction of gases, such as CO, with catalytically active surfaces has been the subject of numerous studies over the past decades. These investigations have increasingly utilized surface spectroscopies that can operate under pressures and temperatures closer to relevant reaction conditions. Such studies are of great consequence since the catalytically active state of a surface in the presence of gases, including the adsorption sites and their relative occupancy, often are not conserved under the ultra-high vacuum conditions (UHV) used in traditional surface science investigations [1,2].

Infrared spectroscopy has been arguably the most widely used method for surface-sensitive investigations of surfaces in the presence of gases. Among the many different versions of IR experiments, infrared reflection absorption spectroscopy (IRRAS) has been commonly used to study vibrational spectra of molecules adsorbed on smooth, IR reflective surfaces at elevated pressures [3–5]. IRRAS allows the distinction of surface species from those in the gas phase by capitalizing on the dipole selection rule, which dictates that surface species interact with *p*-polarized light only. Through comparison of spectra collected using *p*- and *s*-polarized light, contributions from gas phase molecules, which interact with both polarizations, can be removed in pressures up to a few Torr [6]. IRRAS has been used to investigate the adsorption of CO on many single crystalline metal surfaces, including Pd(100), where it has been shown that CO adsorbs in bridge sites [7–10] and there is a linear relationship between the wavenumber and coverage [8]. Coverages in these measurements were determined from low energy electron diffraction (LEED) patterns of characteristic CO surface structures and thermal desorption experiments, measured back-to-back with IR.

Determining CO coverages from combined LEED, thermal desorption, and IRRAS measurements works well under UHV conditions required for the other two techniques. However, the preparation of high CO coverages at or above room temperature requires gas pressures many orders of magnitude higher, inhibiting the use of LEED and thermal desorption. Additionally, IR peak intensities do not always scale linearly with coverage, especially at high coverages where intermolecular interactions are stronger [4]. Under higher pressure conditions, ambient pressure X-ray photoelectron spectroscopy (APXPS) can provide additional quantitative information on the coverage in conjunction with a complete analysis of the elemental and chemical composition of the surface. APXPS utilizes a differentially-pumped lens system to minimize the path length and thus the scattering of the photoelectrons through the gas phase and to separate the experimental cell (typically at pressures up to a few Torr) from the vacuum conditions at the electron detector [11]. APXPS has been applied to study solid/liquid, solid/vapor and liquid/vapor interfaces [12], analogous to IRRAS [6].

A multimodal combined IRRAS and APXPS experiment can provide complementary information on the orientation of adsorbed molecules and their chemical bonding (IRRAS) and the complete elemental profile and chemical environment of the surface (APXPS). The typical sensitivity of 0.01 monolayer of IRRAS (for CO on metals) [5,8] can lead to the identification of species below the XPS detection limit, which is about a few percent of a monolayer. Moreover, the imperative to study increasingly complex chemical environments on surfaces at more

relevant pressures complicates the unambiguous identification of functional groups and surface species by one method alone. Thus the combination of APXPS with IR spectroscopy has been a goal for some time. This multimodal combination is achieved here with the incorporation of IRRAS into the analysis chamber of a synchrotron-based APXPS instrument, with the first combined measurements of CO adsorption on Pd(100) at pressures up to 0.5 Torr.

Materials and Methods

A commercial IR spectrometer (Bruker Vertex 70) was adapted to the APXPS-1 end station [13] at beamline 11.0.2 of the Advanced Light Source [14] at Lawrence Berkeley National Laboratory. The experimental setup is schematically depicted in Fig. 1. Broadband IR light from a Globalar source was first reflected off a planar Au mirror (A). To focus the collimated, 1.8 cm IR beam onto the sample, a series of CaF₂ plano-convex spherical lenses were used. The IR beam was focused with lens B, having a focal length (f) of 200 mm and a diameter (d) of 25.4 mm, and introduced into the analysis chamber through a flange with a KBr window (C, $d=25.4$ mm). This lens focused the diverging beam into the chamber and was found to greatly increase the signal that ultimately made it to the detector. To decrease the focal length, and ideally the spot size on the sample, lenses D ($f=40$ mm, $d=25.4$ mm) and E ($f=20$ mm, $d=12.7$ mm) were separated by minimal distance to focus the IR beam onto the sample with a grazing incident angle of 10° (80° with respect to the sample normal). After reflection, the diverging beam was collimated with lens F ($f=50$ mm, $d=12.7$ mm) and then exited the analysis chamber through a second KBr window (G). Outside the chamber, the light passed through a ZnSe holographic wire grid linear polarizer (H) that was manually rotated between s - and p -polarized light. While positioning the polarizer after the sample was adequate for this study, future experiments will have the polarizer before the sample to control the light that is interacting with the sample. A Au-coated parabolic mirror ($f=43$ mm) focused the light onto a liquid nitrogen cooled mercury cadmium telluride (MCT). A visible component of a tungsten halogen near IR (NIR) source was used for alignment and to determine the approximate size of the IR beam on the sample. Fig. 2 shows this visible light (orange) in relation to the spot probed by XPS (red), which was identified by shining a HeNe laser down the optical axis of the electrostatic lens system and out the differentially-pumped aperture (diameter 0.2 mm).

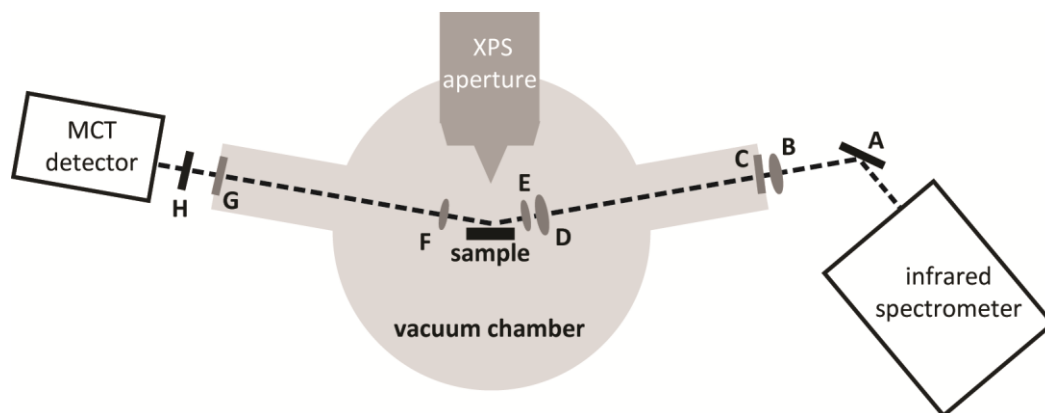


Figure 1. Schematic of the IR beam path (dotted line) through the APXPS analysis chamber. (A) planar gold mirror, (B) lens, $f=200$ mm, $d=25.4$ mm, (C) KBr window in flange, (D) lens,

$f=40$ mm, $d=25.4$ mm, (E) lens, $f=20$ mm, $d=12.7$ mm, (F) lens, $f=50$ mm, $d=12.7$ mm, (G) KBr window in flange, (H) ZnSe polarizer. Lenses are CaF₂. The MCT detector also includes a Au-coated parabolic mirror ($f=43$ mm) to focus the light onto the detector element. The conical aperture to the electrostatic lens of the XPS instrument is shown. Light grey area indicates vacuum areas.

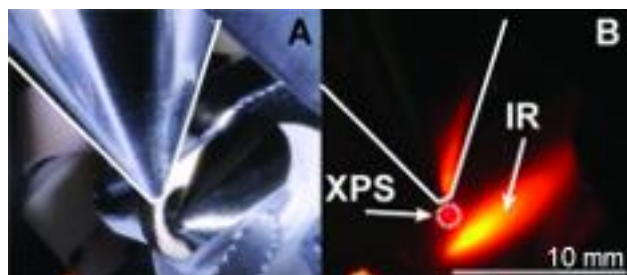


Figure 2. Image of the Pd crystal in front of the aperture illuminated by (a) ambient light and (b) a piece of ceramic in the same position as the Pd crystal illuminated by the visible component of a NIR source used for alignment (orange) and a HeNe laser (red), indicating the XPS measurement position. The rough surface of the ceramic allows for diffuse scattering and visibility of the light sources.

For the optimum IRRAS measurement position (see Figs. 1 and 2) the angle of the incident X-rays on the sample was 20° with respect to the sample normal, and the electron detection angle was $\sim 40^\circ$ to the sample normal. To ensure that the local pressure at the measured sample location is not disturbed by the differentially-pumped aperture, the sample aperture-distance was kept at >2 aperture diameters (>0.4 mm) [11]. The base pressure in the measurement chamber was better than 5×10^{-9} Torr.

A Pd(100) crystal (Surface Preparation Laboratories, Zaandam, Netherlands) was mounted on a pyrolytic boron nitride/pyrolytic graphite heater (PBN/PG, Momentive Performance Materials) with a K-type thermocouple spot welded to the crystal to monitor temperature. The crystal was cleaned by several cycles of Ar⁺ sputtering (1 keV, 3 mA, 2×10^{-5} Torr Ar⁺, 15 min) followed by annealing to 700 °C (10 min). After this initial sample preparation, subsequent sample preparations were performed by heating in 1×10^{-6} Torr O₂ to remove carbonaceous contamination, and, under these conditions, XPS showed the surface to be free of carbon and oxygen. Nevertheless, some adventitious carbon returned while cooling to room temperature at an estimated coverage of less than 0.1 ML (determined from APXPS). The CO gas was passed over heated Cu catalysts (>250 °C) to remove nickel carbonyls. The XPS data were collected with the following photon energies: 490 eV for C 1s, 540 eV for Pd 3d, and 735 for O 1s/Pd 3p. The combined beamline and analyzer resolution was better than 0.35 eV. The C 1s peaks were fit with Doniach-Šunjić functions, where the widths and the asymmetry parameter were constrained to be equal when multiple peaks were used. The IR spectra were collected for 5 min (356 scans) and 4 cm⁻¹ resolution. The *p*-polarization spectrum was divided by the *s*-polarization spectrum, and, subsequently, a polynomial background was removed.

IRRAS data were taken in parallel to the APXPS data, with typical acquisitions times of 10 min for IRRAS and 15 min for a complete APXPS data set.

Results and Discussion

We have tested the feasibility of combined IRRAS/APXPS measurements by studying the adsorption of CO on Pd(100), a system of great interest for a basic understanding of the CO/Pd chemistry in three-way catalytic converters [15]. We first present the IRRAS data. Figs. 3a and 3b show the IR spectrum of CO adsorbed under static CO pressures of 1×10^{-6} Torr and 0.5 Torr CO, respectively. In both spectra, a large peak is observed that corresponds to bridging CO and is known to shift depending on CO coverage [7]. We have estimated the CO coverage in our experiment from previous investigations of the coverage-dependent wavenumber by Ortega and coworkers [8] (see Table 1). CO is known to quickly saturate all two-fold bridging sites to form a 0.5 monolayer (ML) coverage in a $p(2\sqrt{2} \times \sqrt{2})R45^\circ$ structure. Higher coverages can be obtained by rearrangement to a $p(3\sqrt{2} \times \sqrt{2})R45^\circ$ (0.67 ML) or $p(4\sqrt{2} \times \sqrt{2})R45^\circ$ (0.75 ML) structure at higher CO pressures [16] or lower temperatures [7,8]. This former rearrangement is observed in our measurements already at 1×10^{-6} Torr CO with a coverage of 0.65 ML, in agreement with previous results [7]. Increasing the pressure to 0.5 Torr increases the coverage to 0.75 ML, a complete $p(4\sqrt{2} \times \sqrt{2})R45^\circ$ structure. The reversibility of the wavenumber dependence on the coverage is confirmed by heating the sample to 100 °C in UHV, resulting in a peak shift to 1915 cm^{-1} and a 0.20 ML coverage (Fig. 3c). In addition to pure CO adsorption on Pd(100), we have also monitored the influence of NO and O₂ on the CO coverage (Figs. 3d and 3e, respectively). In the case of O₂, surface was first exposed to CO and then O₂ was added to the gas atmosphere. NO is known to bind to Pd, and the CO was introduced after NO to determine the effect of CO displacing an adsorbate. Neither gas was found to have a significant effect on the bridging CO coverage.

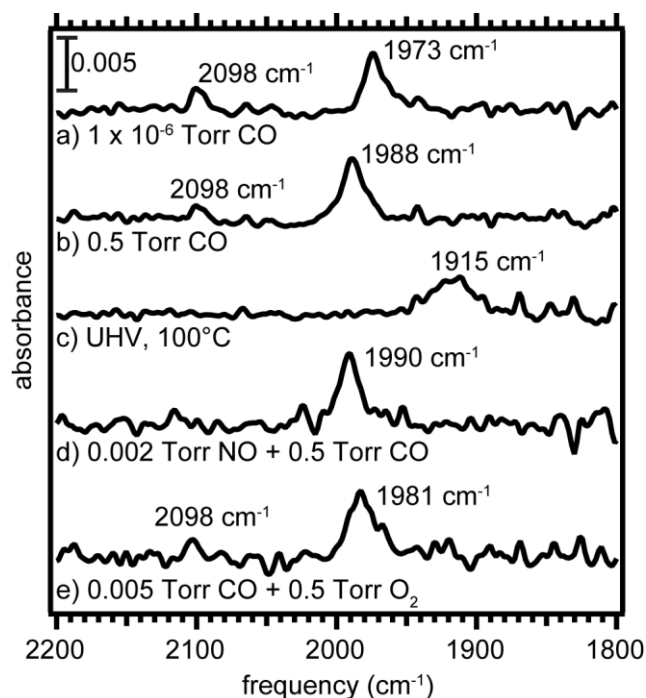


Figure 3. IR spectra of CO adsorbed on Pd(100) under (a) 1×10^{-6} Torr CO, (b) 0.5 Torr CO, (c) UHV conditions at 100 °C after exposure to 1×10^{-6} Torr CO, (d) 0.002 Torr NO & 0.5 Torr CO, (e) 0.005 Torr CO & 0.5 Torr O₂. All spectra were taken at room temperature except (c).

Table 1. CO coverage on Pd(100) from the wavenumber of the bridging CO in the IR spectra and from the intensity in the C 1s XPS data. Coverages obtained by the IR wavenumbers are based on the data by Ortega et al [8]. The errors in the XPS coverage calculations are estimated to be ± 0.06 ML.

condition	Coverage			
	from IR wavenumber	from XPS data		
		total	bridging	atop
1×10^{-6} Torr	0.65	0.61	0.54	0.07
0.5 Torr	0.75	0.91	0.76	0.15
UHV, 100°C	0.20	0.15	0.15	0
0.002 Torr NO + 0.5 Torr CO	0.75	1.0	1.0	0
0.005 Torr CO + 0.5 Torr O ₂	0.70	0.62	0.62	0

A closer inspection of the IR data reveals the presence of a second peak at 2098 cm⁻¹ in Figs. 3a, 3b, and 3e, indicative of CO molecules in the atop position. This species has only been reported on the Pd(100) surface once, to the best of our knowledge, where it was observed at a CO pressure of 1×10^{-7} Torr by Bradshaw et al [7]. They hypothesize that CO quickly fills all the bridging sites on the surface and traps CO molecules momentarily in the atop position [7]. The atop CO peak position is reproducible in our experiments over many cleaning and CO dosing cycles; however, the peak intensity varies each trial, consistent with the previous report [7]. The atop signal is not observed in the case of low CO coverage (Fig. 3c) or when NO was bound to the Pd surface prior to exposure to CO (Fig. 3d). The XPS data indicate that NO adsorbs to the surface at this pressure and is displaced once CO is introduced into the chamber (see Fig. S1), making it less likely that CO molecules will be trapped in atop sites. Under CO and NO gas mixtures, the equilibrium surface coverage is pressure and temperature dependent [17]. Unfortunately, NO was not detected in the IR data, possibly due to the low signal from the small coverage and the overlapping vibrations of background water in the unpurged beam path (see Fig. S2). Fig. 3e shows that the atop species remains upon dosing O₂.

We now turn our attention to the APXPS spectra, which were obtained simultaneously with the IR data. There are a number of previous XPS studies that determined CO coverages on Pd(100) from XPS peak intensities [16,18,19]. One method is based on the relative ratio of the Pd 3d_{5/2} peak components of Pd atoms bound to one bridging CO, CO(I), and Pd atoms bound to two bridging CO molecules, CO(II). The area ratio of CO(II)/CO(I) then indicates the coverage, with the ratio for the $p(3\sqrt{2} \times \sqrt{2})R45^\circ$ structure being 0.5 and that of the $p(4\sqrt{2} \times \sqrt{2})R45^\circ$ structure being 1. The precise determination of this ratio can vary slightly depending on the peak fitting parameters and possible electron scattering effects [18]. In our case, the amount of adventitious carbon could also have contributed to the Pd 3d_{5/2} spectra, which we were not able to fit in accordance with peak parameters given in the literature. These challenges highlight the

need for a second characterization method to complement APXPS, such as IRRAS. Overcoming these challenges, we determined the CO coverage through calculations of a ratio between the total CO area in the C 1s spectra and the total Pd 3d_{5/2} area for each condition. Since all spectra were taken at the same electron kinetic energy, this ratio accounts for effects on the detection sensitivity due to electron scattering in the gas phase and variations in the distance between the aperture and sample [12]. The CO(C 1s)/Pd 3d_{5/2} area ratio at 1 x 10⁻⁶ Torr CO was set to correspond to 0.61 ML, as found previously [7]. The coverages obtained by this procedure are listed in Table 1. Comparing the coverages calculated from IRRAS and APXPS data show good agreement, with the exception of the values at CO pressures of 0.5 Torr. This discrepancy might be explained by the findings of a previous APXPS study of CO on Pd(100), which proposed that a reversible (1 x 1) structure (not verifiable by LEED due to non-UHV conditions) was formed at this pressure [16]. The 1.0 ML coverage from our XPS results agree with this proposal. The literature study of the wavenumber dependence on CO coverage conducted in UHV by Ortega et al. did not extend to coverages beyond 0.8 ML [8], and it is unclear if the wavenumber-coverage relationship is still valid with such a dense coverage. An IRRAS study of Pd(100) did extend the pressure to 1 Torr CO, but they assign the surface coverage to 0.8 ML without confirming the coverage with a second technique (thermal desorption studies were conducted, but only qualitative results are reported) or consideration of a (1 x 1) structure [10]. However, the 1988 cm⁻¹ (Fig. 3b) measured here for the bridging CO at 0.5 Torr matches the 1987 cm⁻¹ reported at 1 Torr [10].

In the following we discuss the possibility to observe CO in atop sites in C 1s XPS spectra. Core level shifts between bridging and atop CO on metal surfaces have been reported in XPS data previously. For example, the O 1s binding energy (BE) of atop CO on Ru(0001) is 1.4 eV higher than that of bridging CO [2]. For Pd substrates, the identification of atop CO from O 1s spectra is complicated by the overlap of the O 1s and Pd 3p_{3/2} peaks. We thus attempt to observe atop CO in the C 1s spectra. Previous measurements of atop CO on Pd(111) have shown that it has a BE 0.55 eV higher than that of bridging CO [20]. Fig. 4 shows C 1s spectra at 1 x 10⁻⁶ Torr CO (bridging + atop, as determined by IRRAS in Fig. 3a) overlaid on the spectrum collected at 60 °C (bridging only, smoothed with 3-point box function), as well as the difference spectrum. Adventitious carbon has a peak at ~284 eV, and the spectrum at elevated temperature shows a coverage of ~0.2 ML. The peak at 285.7 eV is due to bridging CO [16,18]. In addition, a small shoulder at a ~0.5 eV higher BE than the bridging CO peak is visible in the 1 x 10⁻⁶ Torr CO and the difference spectra. The fit parameters of the atop peak are obtained from the difference spectrum; the bottom panel in Fig. 4 shows the C 1s spectrum at 1 x 10⁻⁶ Torr CO fit with both peaks. Two additional data sets in the Supporting Information (Fig. S6) demonstrate reproducibility. From the data in Figs. 4 and S6, the BE of atop CO on Pd(100) is assigned to 286.3 eV ±0.2 eV. In all C 1s spectra at elevated temperatures, this high binding energy peak is absent upon heating, consistent with Bradshaw et al.'s report [7]. There is also no shoulder in the XPS data under the conditions of CO displacing adsorbed NO (Figs. S3 and S4), as confirmed by the IR data in Fig. 3d. Despite the identification of atop CO in IRRAS spectra, previous XPS studies of CO on Pd(100) have not been able to assign a C 1s peak to atop carbon, neither under UHV conditions nor at 0.5 Torr, which was rationalized by the low atop coverage which can be close to the detection limit in XPS. Andersen and coworkers reported a 30 meV increase in the C

1s peak width upon formation of the $p(4\sqrt{2} \times \sqrt{2})R45^\circ$ structure due to the denser packing of the CO [18], but this increase is too small to account for the intensity increase seen here. Without the atop signal in the IRRAS data, adding a second peak to the fit would not be attempted. IRRAS spectra that are obtained simultaneously with XPS, as we have done here, can thus greatly help with the identification of low coverage species if they show high IR activity, as atop CO does.

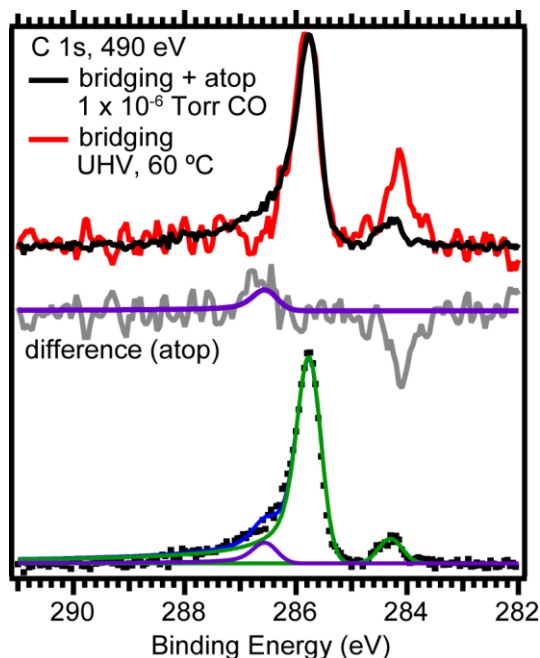


Figure 4. The C 1s spectra of CO adsorbed on Pd(100) under 1×10^{-6} Torr CO (black, bridging + atop) and under UHV at 60 °C (red, bridging). The spectra are normalized to their maximum intensities. The difference between these two spectra are in grey with a Doniach-Šunjić (DS) fit of the difference, which is the peak corresponding to atop CO. The spectrum at 1×10^{-6} Torr CO is fit (blue) with the atop CO peak (purple) in the difference spectrum and a second DS peak (green) for the bridging CO.

In summary, this study represents the first with simultaneous XPS and IR spectroscopy measurements with pressures above UHV and highlights the compatibility of the techniques in identifying peaks in the XPS data. Without evidence of atop CO in the IR data, we would not have identified a C 1s binding energy for this species. Additionally, the coverages calculated from the two techniques are consistent with each other and agree well with previous studies. The increased sensitivity of IRRAS over APXPS could become useful in further closing the pressure gap between APXPS experiments and catalytic reaction conditions. For example, the small amount of CO remaining in an analysis chamber or on the surface during CO oxidation on Pd single crystals is too low to be detected in APXPS experiments [21,22]; IRRAS may be sensitive enough to detect the short-lived, surface-bound CO during reaction conditions.

There is room to improve this first experimental design. The simple amendment of enclosing and purging the beam path outside of the analysis chamber would help with interfering signal from atmospheric gases. For experiments with pressures greater than a few Torr,

polarization modulated IRRAS (PM-IRRAS) can easily be incorporated into the current design to better handle interference from gas-phase absorption. Fig. 2b shows that the areas probed by XPS and IR spectroscopy do not overlap. For use with single crystals where the surface is homogeneous, the lack of overlap is not problematic. However, to continue the trend of investigations of complex materials with APXPS, the IR spot size needs to overlap the sample area illuminated by the X-rays and be reduced to the same magnitude. Such a design would be powerful for examining spatially heterogeneous samples and for probing the effects of photon-induced changes of samples. Reducing the spot size of the IR beam is not trivial. With a Global source, the spot size on the sample is limited by the internal aperture selecting the beam size in the spectrometer. While this aperture can be set to 0.25 mm in the current instrumentation, the intensity of the beam that exits the spectrometer is quite weak. Furthermore, the beam is elongated on the sample surface by the grazing incidence angle. Continuous wave mid-infrared lasers have recently become available, and in principle, can be focused to the diffraction limit of the light. However, the wavelength range with a laser is more limited than with the Global source. Current efforts are underway in all of these areas.

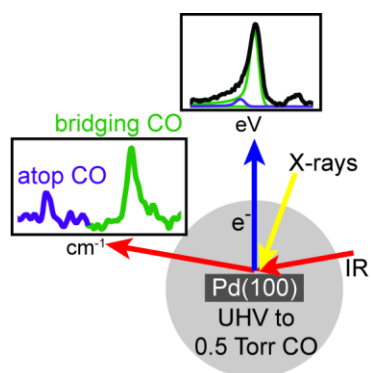
Acknowledgements

The Advanced Light Source is supported by the Director, Office of Science, Office of Basic Energy Sciences, of the U.S. Department of Energy under Contract No. DE-AC02-05CH11231. A.R.H and L.T. acknowledges funding by the Department of Defense, Defense Threat Reduction Agency (Grant HDTRA11510005). H.B., J.R. and T.G. acknowledge support by the Director, Office of Science, Office of Basic Energy Sciences, and by the Division of Chemical Sciences, Geosciences and Biosciences of the U.S. Department of Energy under Contract No. DE-AC02-05CH11231. Bruce Rude is thanked for technical help with the IR instrumentation. Hans Bechtel, Jeff Head, and Niranjana Shivaram are thanked for fruitful discussions on the IR focusing setup.

Appendix A. Supplementary data

Additional APXPS and IRRAS data, including results from additional trials of the experiment, are provided in the Supporting Information. Supplementary data to this article can be found online at

TOC Graphic



Highlights

- Details instrumentation of first combined IRRAS/APXPS study
- IRRAS is essential to identify C 1s binding energy of atop CO on Pd(100)
- CO coverages from IRRAS and APXPS data are consistent with each other

- [1] S. Alayoglu, S.K. Beaumont, G. Melaet, A.E. Lindeman, N. Musselwhite, C.J. Brooks, M.A. Marcus, J. Guo, Z. Liu, N. Kruse, G.A. Somorjai, Surface Composition Changes of Redox Stabilized Bimetallic CoCu Nanoparticles Supported on Silica under H₂ and O₂ Atmospheres and During Reaction between CO₂ and H₂: In Situ X-ray Spectroscopic Characterization, *J. Phys. Chem. C*. 117 (2013) 21803–21809.
- [2] D.E. Starr, H. Bluhm, CO adsorption and dissociation on Ru(0001) at elevated pressures, *Surf. Sci.* 608 (2013) 241–248.
- [3] E.L. Wilson, W.A. Brown, Low Pressure RAIRS Studies of Model Catalytic Systems, *J. Phys. Chem. C*. 114 (2010) 6879–6893.
- [4] F. Zaera, New advances in the use of infrared absorption spectroscopy for the characterization of heterogeneous catalytic reactions, *Chem Soc Rev.* 43 (2014) 7624–7663.
- [5] F. Hoffmann, Infrared reflection-absorption spectroscopy of adsorbed molecules, *Surf. Sci. Rep.* 3 (1983) 107.
- [6] K. Mudiyansele, D.J. Stacchiola, *In-situ* Infrared Spectroscopy on Model Catalysts, in: J.A. Rodriguez, J.C. Hanson, P.J. Chupas (Eds.), *In Situ Characterization of Heterogeneous Catalysis*, John Wiley & Sons, Inc., Hoboken, NJ, USA, 2013: pp. 209–239.
- [7] A.M. Bradshaw, F.M. Hoffmann, The chemisorption of carbon monoxide on palladium single crystal surfaces: IR spectroscopic evidence for localised site adsorption, *Surf. Sci.* 72 (1978) 513–535.
- [8] A. Ortega, F.M. Huffman, A.M. Bradshaw, The adsorption of CO on Pd(100) studied by IR reflection absorption spectroscopy, *Surf. Sci.* 119 (1982) 79–94.
- [9] P. Uvdal, P.-A. Karlsson, C. Nyberg, S. Andersson, N.V. Richardson, On the structure of dense CO overlayers, *Surf. Sci.* 202 (1988) 167–182.
- [10] J. Szanyi, W.K. Kuhn, D.W. Goodman, CO adsorption on Pd(111) and Pd(100): Low and high pressure correlations, *J. Vac. Sci. Technol. Vac. Surf. Films.* 11 (1993) 1969–1974.
- [11] D.F. Ogletree, H. Bluhm, G. Lebedev, C.S. Fadley, Z. Hussain, M. Salmeron, A differentially pumped electrostatic lens system for photoemission studies in the millibar range, *Rev. Sci. Instrum.* 73 (2002) 3872–3877.
- [12] L. Trotochaud, A.R. Head, O. Karshioğlu, L. Kyhl, H. Bluhm, Ambient pressure photoelectron spectroscopy: Practical considerations and experimental frontiers, *J. Phys. Condens. Matter.* 29 (2017) 053002.
- [13] D. Frank Ogletree, H. Bluhm, E.D. Hebenstreit, M. Salmeron, Photoelectron spectroscopy under ambient pressure and temperature conditions, *Nucl. Instrum. Methods Phys. Res. Sect. Accel. Spectrometers Detect. Assoc. Equip.* 601 (2009) 151–160.
- [14] H. Bluhm, K. Andersson, T. Araki, K. Benzerara, G.E. Brown, J.J. Dynes, S. Ghosal, M.K. Gilles, H.-C. Hansen, J.C. Hemminger, A.P. Hitchcock, G. Ketteler, A.L.D. Kilcoyne, E. Kneedler, J.R. Lawrence, G.G. Leppard, J. Majzlam, B.S. Mun, S.C.B. Myneni, A. Nilsson, H. Ogasawara, D.F. Ogletree, K. Pecher, M. Salmeron, D.K. Shuh, B. Tonner, T. Tylliszczak, T. Warwick, T.H. Yoon, Soft X-ray microscopy and spectroscopy at the molecular environmental science beamline at the Advanced Light Source, *J. Electron Spectrosc. Relat. Phenom.* 150 (2006) 86–104.
- [15] E.S.J. Lox, Automotive Exhaust Treatment A list of abbreviations, in: G. Ertl, H. Knözinger, F. Schüth, J. Weitkamp (Eds.), *Handbook of Heterogeneous Catalysis*, Wiley-VCH Verlag GmbH & Co. KGaA, Weinheim, Germany, 2008.

- [16] R. Toyoshima, M. Yoshida, Y. Monya, K. Suzuki, K. Amemiya, K. Mase, B.S. Mun, H. Kondoh, Photoelectron spectroscopic study of CO and NO adsorption on Pd(100) surface under ambient pressure conditions, *Surf. Sci.* 615 (2013) 33–40.
- [17] X. Xu, P. Chen, D.W. Goodman, A Comparative Study of the Coadsorption of carbon monoxide and nitric oxide on Pd(100), Pd(111), and Silica-Supported Palladium Particles with Infrared Reflection-Absorption Spectroscopy, *J. Phys. Chem.* 98 (1994) 9242–9246.
- [18] J. Andersen, M. Qvarford, R. Nyholm, S. Sorensen, C. Wigren, Surface core-level shifts as a probe of the local overlayer structure: CO on Pd(100), *Phys. Rev. Lett.* 67 (1991) 2822–2825.
- [19] R. Toyoshima, M. Yoshida, Y. Monya, K. Suzuki, B.S. Mun, K. Amemiya, K. Mase, H. Kondoh, Active Surface Oxygen for Catalytic CO Oxidation on Pd(100) Proceeding under Near Ambient Pressure Conditions, *J. Phys. Chem. Lett.* 3 (2012) 3182–3187.
- [20] V.V. Kaichev, I.P. Prosvirin, V.I. Bukhtiyarov, H. Unterhalt, G. Rupprechter, H.-J. Freund, High-Pressure Studies of CO Adsorption on Pd(111) by X-ray Photoelectron Spectroscopy and Sum-Frequency Generation, *J. Phys. Chem. B.* 107 (2003) 3522–3527.
- [21] S. Blomberg, M.J. Hoffmann, J. Gustafson, N.M. Martin, V.R. Fernandes, A. Borg, Z. Liu, R. Chang, S. Matera, K. Reuter, E. Lundgren, *In Situ* X-Ray Photoelectron Spectroscopy of Model Catalysts: At the Edge of the Gap, *Phys. Rev. Lett.* 110 (2013).
- [22] R. Toyoshima, M. Yoshida, Y. Monya, Y. Kousa, K. Suzuki, H. Abe, B.S. Mun, K. Mase, K. Amemiya, H. Kondoh, In Situ Ambient Pressure XPS Study of CO Oxidation Reaction on Pd(111) Surfaces, *J. Phys. Chem. C.* 116 (2012) 18691–18697.